Journal of Advanced Marine Engineering and Technology, Vol. 44, No. 4, pp. 274~281, 2020
J. Advanced Marine Engineering and Technology (JAMET)
https://doi.org/10.5916/jamet.2020.44.4.274

ISSN 2234-7925 (Print)
ISSN 2234-8352 (Online)
Original Paper

Development of a 240 kW PEMFC system model for a ship

Eun-Shin Bang[1] · Young-Min Kim[2] · Myoung-Hwan Kim[3] · Sang-Kyun Park[†]

(Received April 6, 2020 ; Revised June 2, 2020 ; Accepted June 30, 2020)

Abstract: In this study, a system model of a marine 240-kW-class fuel cell using oxygen in a liquefied oxygen tank and compressed hydrogen as fuel was developed. The voltage and output characteristic data of the stack according to the change in fuel-cell loads were compared with the experimental results to validate the system. In addition, the system efficiency of the fuel-cell stack, the change in the coolant temperature of the stack, and the discharged-gas temperature on the cathode side were reviewed under various operating loads. As a result, the fuel-cell stack voltage was found to be up to ~4 V below the experimental results in some load areas within the range considered in this study; however, the obtained voltage was almost the same as that observed in the experimental results. The total stack output was calculated to be 250 kW at a maximum load of 530 A, the individual stack efficiency was 59%, and the system efficiency was 53%. Moreover, the PI controller was appropriately operated to maintain an average value of 343 K for the stack coolant temperature from fuel cell No. 1 stack and No. 2 stack.

Keywords: Polymer Electrolyte Membrane Fuel Cell (PEMFC), Performance, Ship, System modeling, Control

1. Introduction

Under the United Nations Framework Convention on Climate Change on Climate Change (UNFCCC), the International Maritime Organization (IMO) conducted discussions on various aspects of reducing greenhouse gases in the international shipping sector. The 72nd Marine Environment Protection Committee (MEPC)-affiliated IMO will attempt at 40% reduction in carbon dioxide emissions from ships by 2030 and 70% reduction by 2050, compared to 2008. This has been approved by the "Initial IMO Strategy on Reduction of GHG Emissions from Ships," in an effort to reduce the annual greenhouse gas emissions of all ships by more than 50% by 2050. The roadmap was established to adopt the final strategy (Revised IMO Strategy) in 2023, by continuing to coordinate the reduction goals and reduction measures of the initial strategy, reflecting possible technological development and trends in greenhouse gas emissions **[1]**. In other words, the shipping industry, which builds and operates ships, prioritizes safety-based environmental issues.

According to the International Transport Forum (ITF) report submitted by the Organization for Economic Co-operation and Development (OECD), the currently used fossil fuels have limited capacity for achieving the reduction targets, and this capacity for reducing the greenhouse gas emissions through linear improvements will increase up to 15% by 2035. For now, the use of LNG fuel is drawing attention. However, it is difficult to meet the mid- and long-term IMO environmental regulations with LNG fuel, and it has been predicted that only 20% reduction in emissions is possible with LNG fuel. Therefore, the replacement of LNG fuel with clean fuel or clean power sources is essential, and 80% of the reduction needs to be replaced by hydrogen or ammonia fuel ships **[2]**. The fuel-cell technology has been developed for land and automobiles, to use hydrogen energy as fuel, and is currently being commercialized. Various research and development projects for applying these fuel-cell technologies to ships have been actively conducted since more than 10 years ago, mainly in Europe **[3]-[8]**. In the short- and medium-to-long terms, a Polymer Electrolyte Membrane Fuel Cell (PEMFC), which is a hydrogen fuel cell currently being commercialized for automobiles, is being considered for the

† Corresponding Author (ORCID: http://orcid.org/0000-0001-9981-6250): Professor, Division of Marine Information Technology, Korea Maritime & Ocean University, 727, Taejong-ro, Yeongdo-gu, Busan 49112, Korea, E-mail: skpark@kmou.ac.kr, Tel: 051-410-4579

1 Ph. D. Candidate, Division of Marine Engineering, Korea Maritime & Ocean University, E-mail: esbang627@kmou.ac.kr, Tel: 051-410-4579

2 Senior Researcher, Electric & Control System R&D Department, Daewoo Shipbuilding & Marine Engineering Co., Ltd. (DSME), E-mail: youngminkim@dsme.co.kr, Tel: 055-735-7146

3 Professor, Division of Marine Engineering, Korea Maritime & Ocean University, E-mail: mhkim@kmou.ac.kr, Tel: 051-410-4267

application of small- and medium-sized ships; actual ship designs are being developed and some small vessels are being built and operated **[9]-[10]**. For the preoccupation of the marine fuel-cell market, additional complementary technologies for securing data and application of ships through mounting the onshore commercialized fuel-cell technology into ships are deemed to be the key. In this respect, although not economically feasible, European countries are believed to have been conducting a continuous demonstration project for more than a decade.

In this study, a system model of a 240-kW-class fuel cell for ships—which uses oxygen in a liquefied oxygen tank and hydrogen in a compressed tank as the fuel, comprising two sets of 120-kW-class stacks—was developed. Then, the voltage and output characteristic data of the fuel-cell stack according to the change in fuel-cell loads were compared with the experimental results. In addition, using the developed model, the stack and system efficiency according to the load, the fuel consumption of the hydrogen and oxygen tanks, the amount of generated water, temperature change of the coolant according to PI control for cooling the fuel-cell stack, and the temperature change of discharged gas from the cathode side were reviewed.

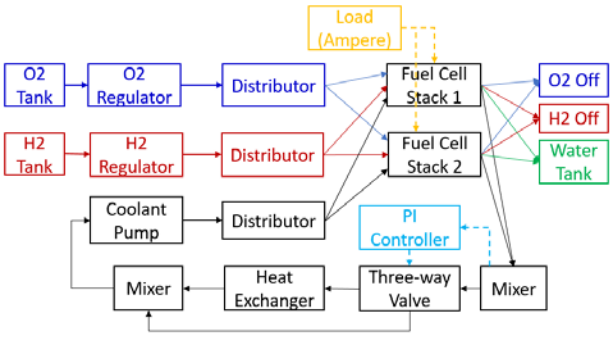

Figure 1: Schematic of the fuel-cell system

2. System Model

2.1 Operating conditions and systems

In this study, Thermolib (Ver. 5.3) and Matlab/Simulink (R2014a) were used to develop the fuel-cell system. **Table 1** shows the specifications of the fuel-cell stack used in this study and its operating conditions. The voltage of a single fuel cell is defined as follows **[11]-[16]**:

$$V_c = E_c - V_{act} - V_{ohm} - V_{con} \quad (1)$$

where V_c represents the voltage per cell (V), E_c represents an open-circuit voltage (V), V_{act} indicates the active voltage loss, V_{ohm} indicates the resistance voltage loss, and V_{con} indicates the concentration voltage loss.

The voltage (V) of the stack is defined as

$$V_{stack} = n \times V_c \quad (2)$$

where n indicates the number of cells. The output (W) of the stack is defined as

$$P_{stack} = V_{stack} \times I \quad (3)$$

where I indicates the current (A). The efficiency (%) of the stack is defined as

$$\eta_{stack} = \frac{V_c}{1.25} \times 100 \quad (4)$$

The efficiency (%) of the fuel-cell system is defined as

$$\eta_{system} = \frac{P_{stack} + P_{stack2} - P_{pump}}{\dot{m}_{H2} \times 30356} \times 100 \quad (5)$$

where $\dot{m}_{H2}$ indicates the hydrogen supply flow rate (kg/s) and P_{pump} indicates the power of the coolant pump.

Figure 1 shows a schematic of the 240-kW-class fuel-cell system developed for ships, which uses hydrogen and oxygen as fuel. Depending on the load input to fuel cell No. 1 stack (Stack 1) and No. 2 stack (Stack 2), the amounts of hydrogen and oxygen that need to be supplied from each tank, as well as the temperature, pressure, and humidity, were regulated through a regulator. The distributor distributed the amounts of hydrogen and oxygen to the stack according to the load input to Stack 1 and Stack 2.

Table 1: Specifications of the fuel-cell system

Parameters	Value
O_2 mass of tank	34,500 kg
Temperature of O_2 tank	90 K
Pressure of O_2 tank	3,749,025 Pa
H_2 mass of tank	57.3 kg
Temperature of H_2 tank	318 K
Pressure of H_2 tank	6,484,800 Pa
Stoichiometric ratio of O_2	2
Stack supply temperature of O_2	343 K
Stack supply pressure of O_2	253,313 Pa
Stack supply humidity of O_2	100%
Stoichiometric ratio of H_2	1.2
Stack supply temperature of H_2	318 K

Stack supply pressure of H_2	253,313 Pa
Stack supply humidity of H_2	100 %
Number of cells(Stack 1)	320
Number of cells(Stack 2)	320
Active area	0.16 m^2
Membrane thickness	0.0003 m
Target temperature of coolant	343 K
Coolant flow rate	3.68 kg/s
Outlet pressure of coolant pump	405,300 Pa

The water generated from the fuel cell was collected in the water tank. The coolant with the fixed value flow rate and temperature was supplied to each fuel-cell stack through the distributor at the coolant pump outlet regardless of the load on Stack 1 and Stack 2. A PI controller was installed to maintain an average temperature of 343 K for the stack coolant in the mixer, where the stack coolant outlet side from Stack 1 and Stack 2. The stack coolant temperature of this mixer was regulated by controlling the by-pass amount of stack coolant entering the heat exchanger from the 3-way valve operated on input signal of the PI controller. The heat exchanger was cooled by the seawater of constant flow rate and temperature, with a counter flow.

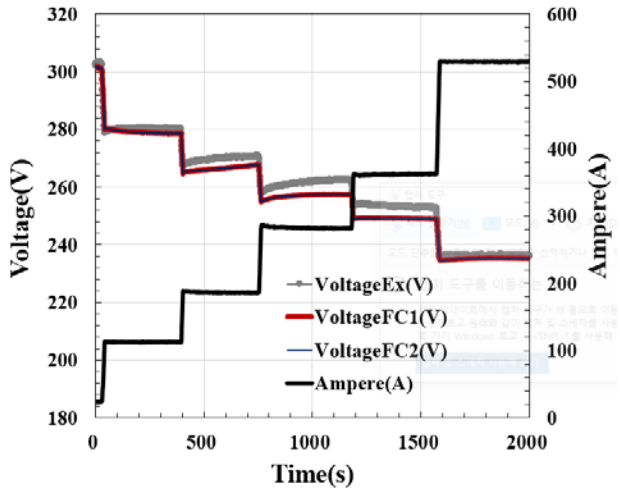

Figure 2: Comparison of the stack voltage between the experiment and simulation

3. Analysis Result

Figure 2 shows a graph comparing the experimental (VoltageEx) and calculation (VoltageFC1, VoltageFC2) results of the stack voltage with the load (A) of the fuel-cell stack varying with time. When evaluating the fuel-cell system model, the change in load over time was entered in Stack 1 and Stack 2 with the same load as that used in the experiment. There was no difference in the calculation results of the voltages of Stack 1 and Stack 2 with varying loads, and the calculation results were almost identical to the experimental results in the full-load area. There were load areas where the calculation results of up to ~4 V were lower than the experimental results. However, a difference of ~0.01 V per cell in terms of a single cell's voltage should be considered for the effect of the part that cannot be expressed in the calculation under certain conditions, such as the experimental conditions.

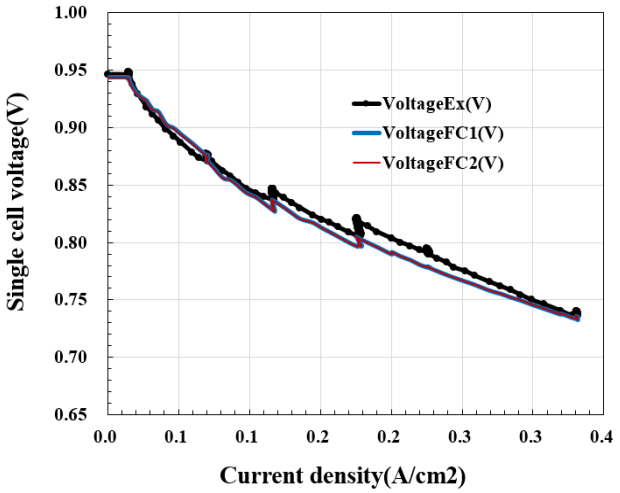

Figure 3: Comparison of the average single-cell voltage between the experiment and simulation

Figure 3 represents the average voltage of a single cell according to the current density. At a current density of ~0.2 A/cm^2, the experimental and calculation results had a maximum voltage difference of ~0.01 V. In addition, the stack voltage decreased as the load increased. This was because, as shown in the graph in **Figure 4**, the current density and average overvoltage for a single cell of Stack 1 increased the activation overvoltage (ActFC1) and Ohmic overvoltage (OhmFC1) as the load increased. In this study, the load area showed a little concentration overvoltage (CocnFC1).

Figure 5 shows the stack power, stack efficiency, and system efficiency under the same conditions as those presented in **Figure 2**. The stack output in the overall load area showed that the experimental results (PowerEx) and calculation results (PowerFC1) were almost identical. Especially, the output of one stack could be obtained at ~125 kW and the combined output of

both stacks was ~250 kW at load 530 A. At this time, the calculation result for each stack efficiency was ~59% and the system efficiency was calculated by subtracting the power required to drive the stack coolant pump from the output of the two fuel-cell stacks, which was ~53% of the calculation result.

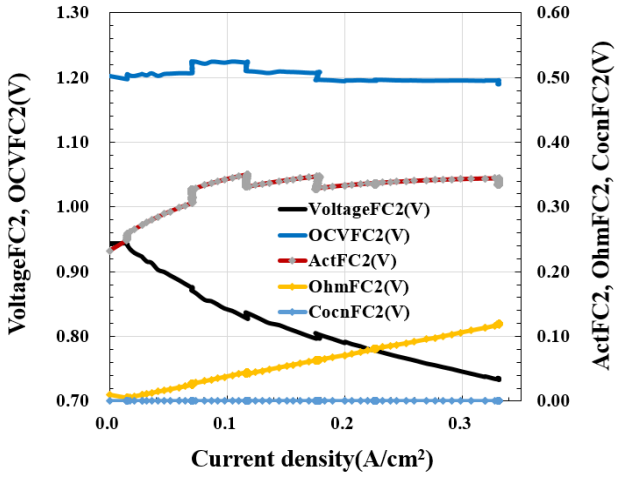

Figure 4: Characteristics of the open-circuit voltage and over-voltage for a single cell

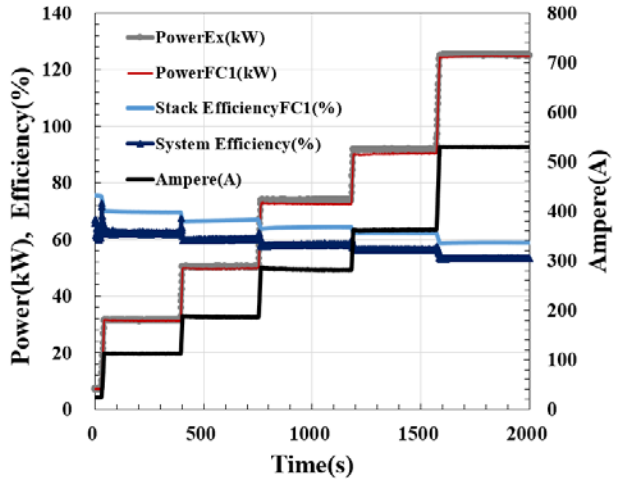

Figure 5: Comparison of the stack voltage between the experiment and simulation

Figure 6 shows the amounts of fuel remaining in a hydrogen tank (H_2Tank) and an oxygen tank (O_2Tank) depending on operations of Stack 1 and Stack 2, as well as the amount of change in the generated water (WaterTank) over time under the fuel-cell operation. Approximately 4 kg hydrogen was consumed, ~57 kg oxygen was consumed, and ~36 kg water mass was generated.

Figure 7 shows the stack coolant inlet temperature (HeatIN) entering the heat exchanger under the same conditions as those presented in **Figure 2**, the stack coolant outlet temperature (HeatOUT) exiting the heat exchanger, and the temperature of the gas emitted on the cathode side (CatOUTTemp) from the fuel-cell stack.

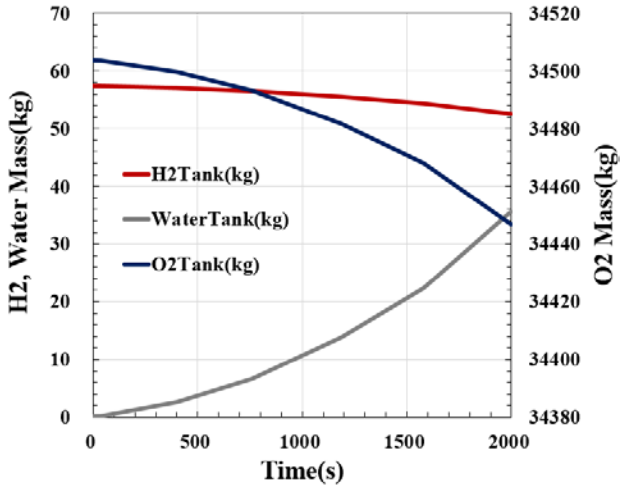

Figure 6: Characteristics of changes in fuel mass and generator water mass with time

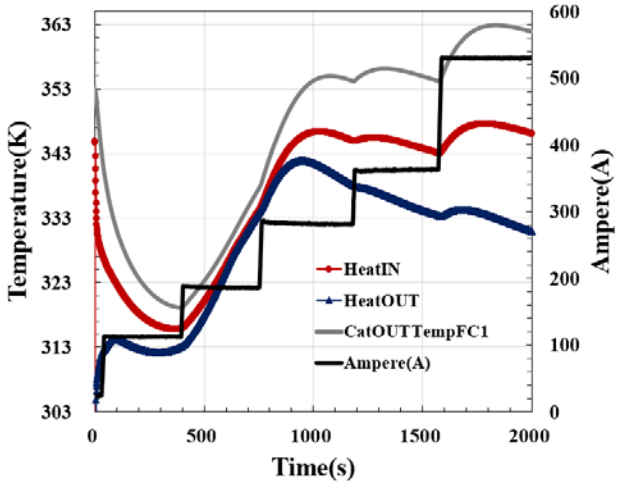

Figure 7: Characteristics of inlet and outlet coolant temperatures for heat exchanger

The operation of the fuel-cell system indicated that the HeatIN entering the heat exchanger was lower than the PI controller's setting temperature of 343 K, because the amount of heat generated in the fuel-cell stack was not sufficient for reaching the area with a low load of 185 A. In addition, the stack coolant was by-passed without entering the heat exchanger. This is because the HeatOUT was approximately equal to the HeatIN. At a load above 281 A, the HeatIN was higher than the

PI controller's setting temperature of 343 K, and thus, the amount of stack coolant entering the heat exchanger increased. As the load increased, the temperature difference between the stack cooling water entering the heat exchanger and the stack coolant cooled by the heat exchanger increased. At 2000 s, the HeatIN was 346 K, the HeatOUT was 331 K, and the CatOUTTemp was 362 K.

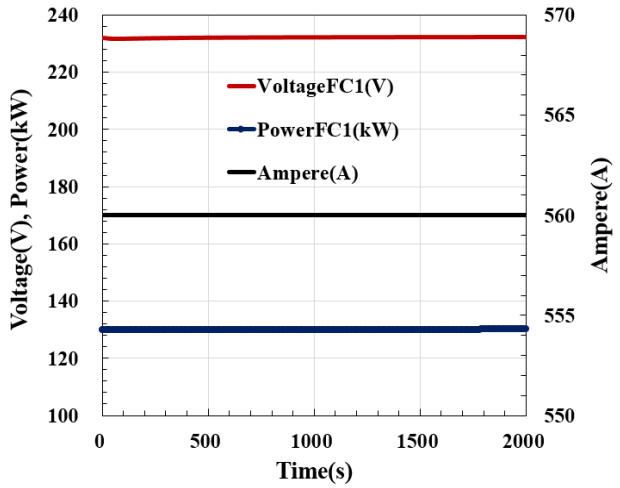

Figure 8: Characteristics of voltage and power with time

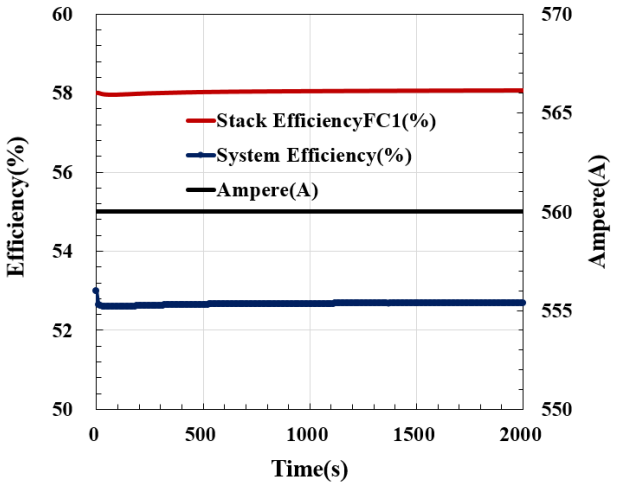

Figure 9: Characteristics of stack efficiency and system efficiency with time

Figure 8 shows the calculation results of the stack voltage (VoltageFC1) and output (PowerFC1) at a constant load of 560 A for each fuel-cell stack. The calculation results obtained for Stack 1 and Stack 2 were the same, and thus, only the value of Stack 1 was presented. The stack voltage was ~232 V and the output was ~130 kW; the output sum of both was ~260 kW.

Figure 9 shows the stack efficiency and system efficiency when the load of each fuel-cell stack was maintained constant at 560 A.

The calculation results obtained for Stack 1 and Stack 2 were the same, and thus, only the value of Stack 1 was presented.

The stack efficiency was ~58% and the system efficiency, which was obtained by subtracting the power required to drive the stack coolant pump from the sum of the outputs Stack 1 and Stack 2, was ~53%.

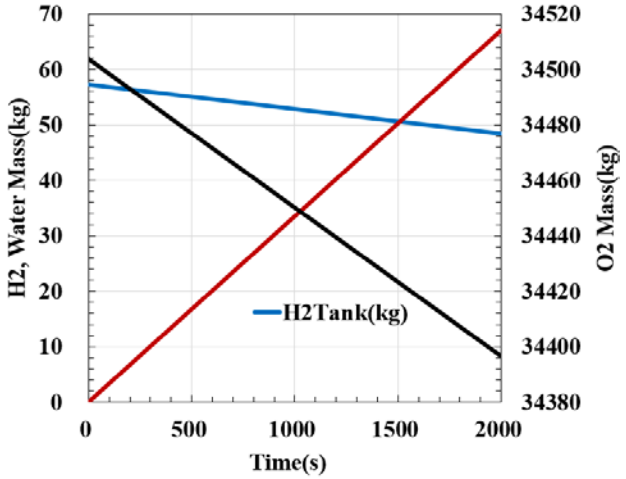

Figure 10: Characteristics of changes in fuel mass and generator water mass with time

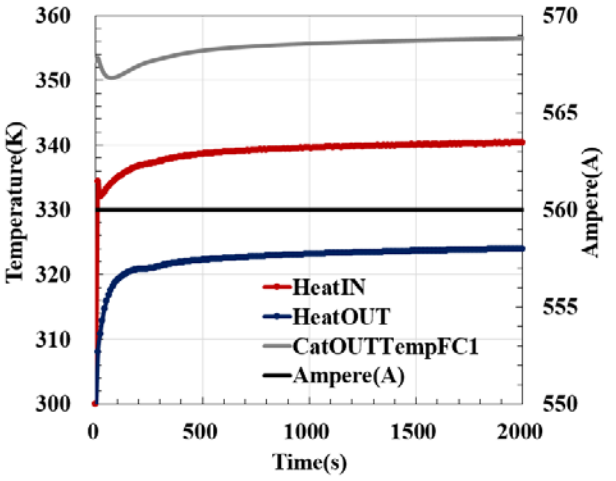

Figure 11: Characteristics of HeatIn and HeatOut

Figure 10 shows changes, over time, in the amounts of fuel remaining in H_2Tank and O_2Tank and the water mass generated by the operation of the fuel cell according to the operation of Stack 1 and Stack 2. Approximately 9 kg hydrogen was consumed, ~108

kg oxygen was consumed, and ~67 kg water mass was generated.

Figure 11 shows the HeatIN, HeatOUT, and CatOUTTemp under a constant load of 560 A for each fuel-cell stack. At 2000 s, the HeatIN was maintained at 340 K and the HeatOUT was maintained at 324 K as the rate of stack coolant flow into the heat exchanger was controlled according to the PI controller signal. At this point, the CatOUTTemp was 356 K, indicating a temperature difference of ~16 K from the HeatOUT. The PI controller operated appropriately for maintaining an average HeatIN of 343 K from Stack 1 and Stack 2.

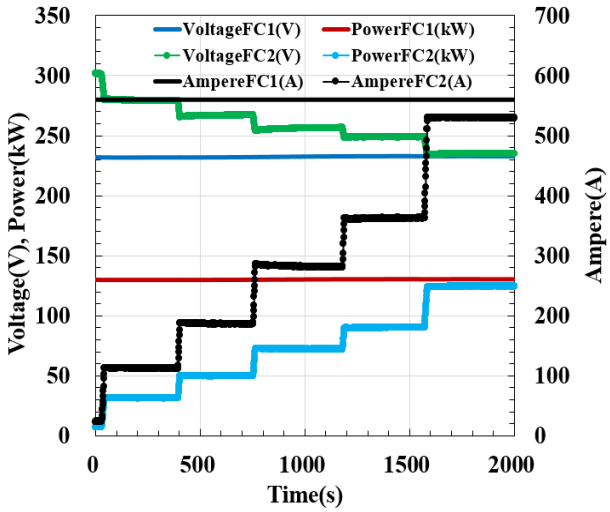

Figure 12: Characteristics of voltage and power with time

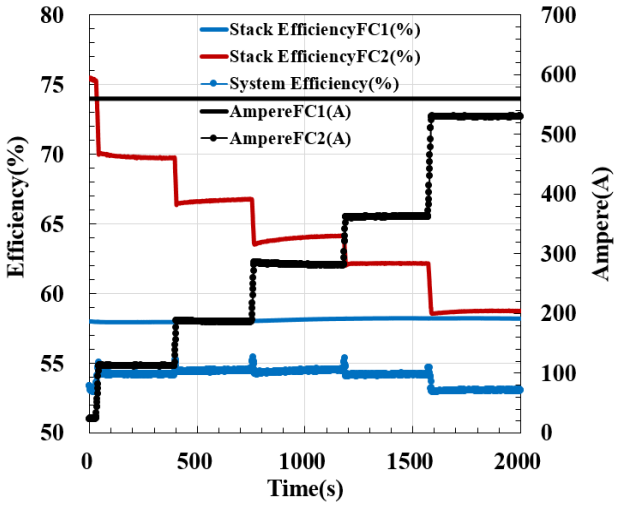

Figure 13: Characteristics of stack efficiency and system efficiency with time

Figure 12 shows the calculation result of each stack voltage and output at a constant load of 560 A for Stack 1 and varying load for Stack 2 over time. Stack 1 maintained a constant output, while Stack 2 showed changes in the output with load variations.

Figure 13 shows the stack efficiency and system efficiency at a constant load of 560 A for Stack 1 and varying load, with time, for Stack 2. Stack 1 exhibited a constant stack efficiency, while Stack 2 showed a decrease in the stack efficiency with an increase in load. The system efficiency reduced as the load increased, with the total output of Stack 1 and Stack 2 subtracted from the power consumed by the stack coolant pump.

Figure 14 shows the change, over time, in the amount of fuel remaining in H_2Tank and O_2Tank according to the operation of Stack 1 and Stack 2, and the amount of water generated by the operation of the fuel cell (WaterTank). Approximately 6 kg hydrogen was consumed, ~82 kg oxygen was consumed, and ~51 kg water mass was generated.

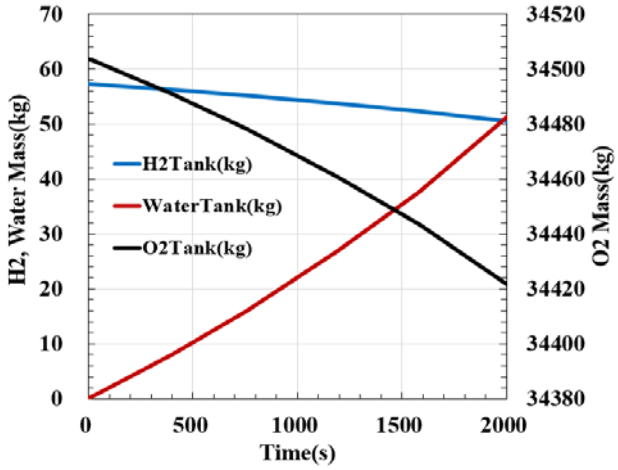

Figure 14: Characteristics of changes in fuel mass and generated water mass with time

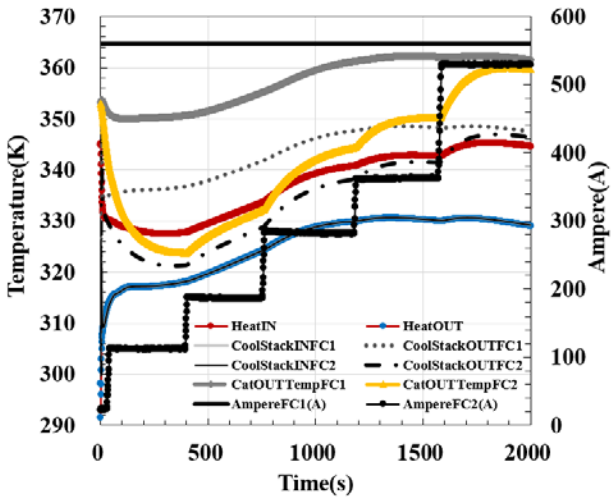

Figure 15: Characteristics of HeatIN and HeatOUT

Figure 15 shows HeatIN, HeatOUT, and CatOUTTemp exiting from the fuel-cell stack when the load of Stack 1 was maintained constant at 560 A, while that of Stack 2 was changed over time. The stack was supplied with coolant at the same flow rate and temperature (HeatOUT Temperature=CoolStackInFC1=CoolStackInFC2), regardless of the load, to Stack 1 and Stack 2.

The stack coolant outlet temperature of Stack 1 (CoolStackOUTFC1), which had a high load of 560 A, was higher than the stack coolant outlet temperature of Stack 2 (CoolStackOUTFC2). The cathode exhaust gas outlet (CatStackOUT) changed with the same trend as the stack cooling water outlet temperature (CoolStackOUT), and its difference from CoolStackOUT increased with the load. CoolStackOUTFC1 with high load was higher than CoolStackOUTFC2. The combined coolant outlet flow of Stack 1 and Stack 2 was HeatIN. In the low-load region, if the flow rate of the cooling water is controlled as a method for reducing the power consumption of the pump, the system efficiency can be improved.

4. Conclusion

This study developed a system model of a marine 240-kW-class fuel cell using oxygen in a liquefied oxygen tank and compressed hydrogen as fuel. The voltage and output characteristic data of the fuel-cell stack according to the change in fuel-cell loads were compared with the experimental results to validate the system. In addition, the system efficiency of the fuel-cell stack, the change in the coolant temperature for the stack, and discharged-gas temperature on the cathode side were reviewed under varying operating loads.

(1) The calculation results of the fuel cell stack voltage with varying loads showed up to ~4 V below the experimental results in some load areas, but could simulate voltage characteristics similar to those of the experimental results.

(2) A combined output of ~250 kW could be obtained from the maximum load of 530 A under the experimental conditions, which was the rated load. The stack efficiency was shown to be ~59% and the fuel-cell system efficiency considering the power required to drive the coolant pump was ~53%.

(3) The consumption of liquefied air and compressed hydrogen, depending on the load of the fuel-cell stack, and the generated water mass, resulting from the chemical reaction of the fuel cell, could be implemented.

(4) The PI controller for controlling the flow rate of the stack outlet coolant entering the heat exchanger, introduced to maintain a constant stack coolant outlet temperature, was appropriately operated.

(5) In the low-load area, the power consumption of the pump is related to the system efficiency; thus, if the flow rate control of the coolant pump is made to reduce the flow rate of the coolant at a low load, it is judged to be advantageous in terms of system efficiency.

Acknowledgements

This study was conducted with the support of Daewoo Shipbuilding & Marine Engineering Co., Ltd.'s “Improving Ship Energy Efficiency” R & D project.

Author Contributions

Conceptualization, S. K. Park; Methodology, S. K. Park and E. S. Bang; Software, E. S. Bang; Formal Analysis, M. H. Kim; Investigation, All Authors; Resources, All Authors; Data Curation, E. S. Bang; Writing-Original Draft Preparation, S. K. Park and E. S. Bang; Writing-Review & Editing, E. S. Bang; Supervision, S. K. Park; Project Administration, S. K. Park and Y. M. Kim; Funding Acquisition, Y. M. Kim.

References

[1] American Bureau of Shipping (ABS), MEPC 72 Brief, https://ww2.eagle.org/content/dam/eagle/regulatory-news/2018/MEPC%2072%20Brief%20FINAL.pdf, Accessed August 8 2020.

[2] Transport: Pathways to zero-carbon shipping by 2035 (Case-Specific Policy Analysis), https://www.itf-oecd.org/sites/default/files/docs/decarbonising-maritime-transport-2035.pdf, Accessed August 5 2020.

[3] E. Fontell, “Wärtsilä fuel cell development program,” The 8th Annual Green Ship Technology Conference, 2011.

[4] Energy Observer Project, http://www.energy-observer.org, Accessed September 02, 2019.

[5] E4ship Project, http://www.e4ships.de, Accessed September 02, 2019.

[6] C. H. Choi, S. J. Yu, I. S. Han, B. K. Kho, D. G. Kang, H. Y. Lee, M. S Seo, J. W. Kong, G. Y. Kim, J. W. Ahn, S. K.

Park, D. W. Jang, J. H. Lee, and M. J. Kim, “Development and demonstration of PEM fuel-cell-battery hybrid system for propulsion of tourist boat,” International Journal of Hydrogen Energy, vol. 41, no. 5, pp. 3591-3599, 2016.

[7] M. H. Kim, “Analysis on the technology R&D of the fuel cell systems for power generation in ships,” Journal of the Korean Society of Marine Engineering, vol. 31, no. 8, pp. 924-931, 2007 (in Korean).

[8] EMSA European Maritime Safety Agency, Study on the Use of Fuel Cells in Shipping, DNV GL, Germany, 2017.

[9] J. W. Pratt and L. E. Klebanoff, Feasibility of the SF-BREEZE: a Zero-Emission, Hydrogen Fuel Cell, High-Speed Passenger Ferry, SANDIA REPORT (SAND2016-9719), Sandia National Laboratories, U. S., 2016.

[10] J. W. Pratt and L. E. Klebanoff, Optimization of Zero Emission Hydrogen Fuel Cell Ferry Design, With Comparisons to the SF-BREEZE, SANDIA REPORT (SAND2018-0421), Sandia National Laboratories, U. S., 2018.

[11] J. Larminie and A. Dicks, Fuel Cell Systems Explained, John Wiley & Sons, 2003.

[12] J. T. Pukrushpan, Modeling and Control of Fuel Cell Systems and Fuel Processors, Ph. D. Dissertation, Mechanical Engineering, University of Michigan, USA, 2003.

[13] J. I. Kim and S. K. Park, “Development of a 120kW PEMFC stack model for a ship vessel,” Journal of the Korean Society of Marine Engineering, vol. 43, no. 7, pp. 492-497, 2019 (in Korean).

[14] J. T. Pukrushpan, A. G. Stefanopoulou, and H. Peng, Control of Fuel Cell Power Systems: Principles, Modeling, Analysis and Feedback Design, Springer-Verlag London, 2005.

[15] EUtech Scientific Engineering, Simulation toolbox for the design and development of thermodynamic system in MATLAB/Simulink, 2009.

[16] F. P. Incropera, D. P. Dewitt, T. L. Bergman, and A. S. Lavine, Fundamentals of Heat and Mass Transfer, 6th edition, John Wiley & Sons, 2008.